

Attenuation with distance and wind speed of HF surface waves over the ocean

P. Forget, P. Broche, and J. C. de Maistre

Laboratoire de Sondages Electromagnétiques de l'Environnement Terrestre, Université de Toulon
83100 Toulon, France

(Received July 30, 1981; revised November 4, 1981; accepted November 4, 1981.)

An HF monostatic experiment is performed in order to evaluate the relative attenuation with distance of radio waves propagating in the ground wave mode over the sea surface, at 7 and 14 MHz. Clear evidence of the wind speed (causing the sea roughness) influence arises from the data, particularly at 14 MHz. The results are compared to Barrick's theoretical calculations, and a good agreement is found for the values of attenuation rates (in decibels per kilometer) and their variation with the wind speed in the upwind/downwind case. Some discrepancies in the data are partially interpreted as due to a fetch influence upon the radar cross section.

1. INTRODUCTION

The existence of a ground wave mode for radio waves propagating over the ocean has been known for a long time. There are many papers about this problem, but only a few of them tackle it from a purely experimental standpoint and, in particular, are devoted to the experimental evaluation of ground wave attenuation with distance and with the roughness of the sea state. The transmission loss is rather important (say 30–70 dB for 100 km at HF), so that the ground wave mode is rarely used in radio transmission systems at HF in comparison with the ionospheric (sky wave) mode, which allows much longer ranges. Nevertheless, there are some practical reasons for knowing the ground wave attenuation rate with distance and with respect to the sea roughness, and one of them, apart from communication problems, lies in the capabilities of ground wave HF radars for sea state remote sensing (ocean waves and surface currents). This technique has been used for a decade (for recent reports, see Frish and Weber [1980], Lipa and Barrick [1980], Stewart and Teague [1980], Trizna et al. [1980], and Forget et al. [1981]) on the basis of theoretical works [Barrick, 1972] for the interpretation of the sea echo Doppler spectrum.

Since the expected wave information is theoretically contained in the radar cross section (RCS),

which depends only upon the radar frequency and the properties of the target, each study implying observations at different distances from the radar needs knowledge of the ground wave transmission loss. For instance, Stewart and Teague [1980] made measurements of ocean wave growth and decay by observing radar sea echoes from 20 to 200 km, the signals being corrected by a law in $1/R^3$ in order to remove the attenuation of HF waves with distance. The more complete theoretical results presented up to now are those of Barrick [1970, 1971a, b]. The author gives the ground wave attenuation above the sea surface and takes into account the earth's curvature and the effect of the roughness due to ocean waves. The results are briefly described in section 2.

Experimental measurements of transmission loss over the ocean have been made by Hansen [1977] with two distant stations, at frequencies from 4 to 32 MHz. They generally agree with the theory in the limit of the wind velocities encountered, below 17 kn (8.7 m/s).

The present paper reports the results of an HF monostatic experiment giving significant variations with distance (up to 100 km) and wind conditions (5–38 kn (2.6–19.6 m/s)) of the backscattered signals. The principles developed in section 3 explain how monostatic measurements can be used to determine relative ground wave attenuations. Experimental results (section 5) are compared with Barrick's theoretical ones, and an attempt is made to relate some of them, associated with special wind conditions, to an effect of the fetch.

2. THEORETICAL VALUES OF GROUND WAVE ATTENUATION

For a monostatic configuration the received power may be written as

$$P_R = \alpha \lambda^2 (F^2/R^2)^2 \sigma dS \quad (1)$$

where α is a constant term including the transmitted power, antenna gains, and system losses; λ is the electromagnetic wavelength; R is the distance of observation of the sea cell whose area is dS ; and σ is the RCS. F^2 is the Norton attenuation factor for the energy, relative to a one-way path between the radar and the sea cell. The exponent 2 of $(F^2/R^2)^2$ is due to the double path of em waves radar-to-target and target-to-radar.

According to the theory the boundary condition calls for F to approach unity when R approaches zero. F depends upon the distance R and the sea surface impedance (including the roughness effect) and describes the difference between a propagation above a smooth, plane, and perfectly conductive ground and a propagation above a curved and rough medium of finite conductivity. In the first case, the power decreases with a law in $1/R^2$, and the Norton factor is equal to 1; in the second case, F is less than unity, and the power decreases with distance following a law as $F^2(R)/R^2$.

For a one-way path of em waves the total attenuation is described by Barrick using the concept of 'basic transmission loss' L_b , which is $L_b = -10 \log l_b$ where l_b is a nondimensional quantity equal to $\lambda^2 F^2 / 4\pi^2 R^2$. L_b can be seen as the ratio between the powers radiated and received respectively by two isotropic antennas at distance R one from the other.

For monostatic experiments it is convenient to use the 'monostatic basic transmission loss,' defined as

$$L_{bm} = 2L_b \quad (\text{or } l_{bm} = l_b^2)$$

The variations of L_{bm}^0 , where the superscript 0 refers to a smooth sea surface, are derived from Barrick's L_b curves and are shown in Figure 1. The water conductivity is 4 mhos/m.

The influence of the sea state consists of a term ΔL_{bm} (in decibels) which has to be added to L_{bm}^0 and is equal to zero when the sea surface is smooth. Some values of ΔL_{bm} are shown in Table 1. They are derived from Barrick's calculations and concern two radar frequencies, 7 and 14 MHz.

Three models for the wave spectrum are considered. The first two are Neumann-Pierson (N-P) spectra with a cosine squared directionality factor

($\cos^2 \theta$, where θ is the angle referred to the mean orientation of the wave field); the wind is blowing in directions parallel to the radar beam (upwind or downwind) and perpendicular (cross wind), respectively. The third one is a Phillips spectrum with an isotropic distribution of waves. It must be noted that the wave motions are unimportant for these calculations (as if the sea was 'frozen' during the travel time of radio waves); in other words the directionality factor applies to the slopes of the ocean waves encountered by radio waves.

ΔL_{bm} increases with the radar frequency and the distance. For the cosine squared model, ΔL_{bm} has higher values in the upwind/downwind case than in the cross-wind case; the greater the amount, the higher the frequency.

Thus the sensitivity of ground wave attenuation to wind direction remains, in absolute value, larger at high frequencies than at low frequencies. Lastly, the isotropic model leads, in general, to intermediate values of ΔL_{bm} between those corresponding to cross wind and radial wind for the anisotropic model.

3. PRINCIPLES OF THE MEASUREMENTS

The possibility of measuring the ground wave attenuation with distance with a monostatic radar system lies in the properties of the radar cross section σ , appearing in (1). The theory at first order of interactions between radio waves and sea waves [Barrick, 1972] shows that σ is proportional to the total energy of the two spectral components, along the radar beam axis, of these waves whose wavelength is half the radio wavelength ('Bragg waves'). The other waves are involved in the mechanism through second-order effects, the influence of which on the total power return may be considered as negligible. If f_B , k_B are the frequency and wave number of the ocean waves involved in the first-order scatter and if f_0 , k_0 are the radar frequency and wave number, one has

$$k_B = 2k_0$$

$$f_B \text{ (Hz)} = 0.102 [f_0 \text{ (MHz)}]^{1/2} \quad (2)$$

$$\sigma \sim S(f_B) [\phi(\pi - \theta) + \phi(\theta)]$$

S is the usual frequency wave spectrum; θ is the angle between the radar beam axis and the mean direction of the f_B wave field; and $\phi(\alpha)$ is the directionality factor of the wave spectrum, reaching its extrema when $\alpha = 0$ or π . When direct evaluations of the wave spectrum by standard sensors are not avail-

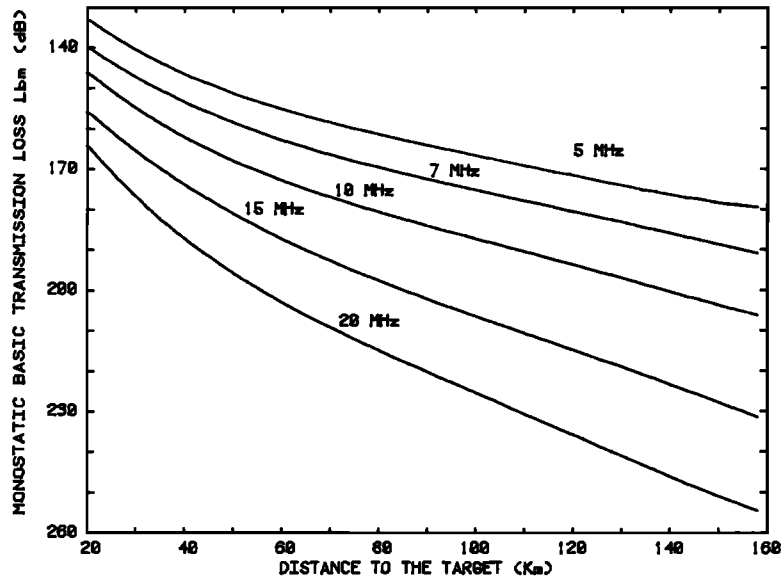


Fig. 1. Monostatic basic transmission loss L_{bm}^0 at HF; the sea surface is smooth [from *Barrick*, 1971b].

able, an exact knowledge of the RCS is not needed if the experimental conditions are such that σ can be supposed to be the same at each distance of observation; this means that the sea is homogeneous all over the zone covered by the radar.

These conditions are assumed to be realized if the following two criteria are fulfilled:

1. The wind is blowing from offshore, and it has a speed high enough to saturate the waves responsible for the first-order radar sea echo everywhere

TABLE 1. Added monostatic transmission loss for a rough sea (in decibels), where three distances of the radar cell, three wind velocities, two wind directions, and two models for the directional sea spectrum are considered (Neumann-Pierson and Phillips isotropic).

	Values at 7 MHz			Values at 14 MHz		
	N-P radial wind	N-P cross wind	Phillips isotropic	N-P radial wind	N-P cross wind	Phillips isotropic
20 km						
10 kn (5.1 m/s)	-0.3	-0.2	-0.7	0.4	0	0.1
20 kn (10.3 m/s)	0.5	0	0	3.4	0.6	2.5
30 kn (15.4 m/s)	2.5	0.5	1.1	9.4	2	4.8
60 km						
10 kn (5.1 m/s)	-0.3	-0.2	-0.8	.9	0.1	1.7
20 kn (10.3 m/s)	1.4	0.3	1	9.2	1.6	8.4
30 kn (15.4 m/s)	6.6	1.8	3.2	22.2	5.4	14
100 km						
10 kn (5.1 m/s)	-0.3	-0.2	-1	1.9	0.1	3.6
20 kn (10.3 m/s)	2.7	0.4	2	13.6	2.7	12.5
30 kn (15.4 m/s)	10.6	2.9	5.2	28.6	8.2	19.5

N-P is Neumann-Pierson. Data are from *Barrick* [1970].

within the radar coverage area. By taking a Pierson and Moskowitz (P-M) spectrum the spectral energy $S(f_B)$ is then equal to $(2\pi)^{-4} \beta_e g^2 f_B^{-5}$, where g is the gravity and β_e , the Phillips saturation parameter, is a constant with an order of magnitude of 10^{-2} [Phillips, 1977].

2. The wind direction is the same for every distance of observation; this can be evaluated with the help of the ratio of the first-order lines in the radar sea echo Doppler spectrum, which are proportional to the spectral energy of the receding and approaching Bragg waves, respectively. This ratio is then equal to $\phi(\theta)/\phi(\pi - \theta)$ and, for a given value of f_B and a given shape for ϕ , depends only upon θ , the dominant wave field direction referred to the radar beam axis.

Concerning point 1, $S(f_B)$ is almost independent of the long-period part of the spectrum if F_m , the dominant wave frequency, is much less than f_B . For a fully developed sea where waves of frequency F_m move with nearly the same speed as the wind, this condition between F_m and f_B can be written as $g/2\pi U \ll f_B$ (U is the wind speed), so by using (2) we have U (m/s) $\gg 15.3/[f_0$ (MHz)]^{1/2}. Then, at 7 and 14 MHz the wind velocity must be greater than 6 and 4 m/s, respectively.

Points 1 and 2 being satisfied, the determination of ground wave attenuation simply consists in measuring the spectral energy of the first-order lines as a function of distance. Obviously, it is not possible to get directly from this mean absolute values of L_{bm} that can be compared to those predicted by the theory. Returning to (1), the backscattered power is seen to be weighted by the law in $1/R^4 \times dS$ which becomes $1/R^3$ since dS is determined by the aperture angle of the radar beam and therefore is proportional to the distance R . That law being true and not specific to the ground wave mode of propagation, it is more illustrative to study the variation with R and the wind parameters of the relative monostatic Norton attenuation factor, say N_{mr} , given by

$$N_{mr} = 10 \log P_R \cdot R^3 - 10 \log \sigma \quad (3)$$

By assuming σ to be constant, N_{mr} would be constant (independent of R) for propagation in free space or over a smooth, plane, and perfectly conductive sea surface.

From N_{mr} one gets the global attenuation loss under the form of the relative monostatic basic transmission loss L_{bmr} by

$$L_{bmr} = -N_{mr} + 40 \log R \quad (4)$$

4. THE EXPERIMENT

An HF experiment was undertaken between March 23 and April 2, 1981, near Marseille (France). The radar used, for transmission, a biconical antenna radiating HF waves in the range 5–20 MHz. The backscattered electric field is received on a linear array of 16 monopole antennas. The electronic processing and recording devices are located in a laboratory van.

The transmitted wave is pulsed at a rate of 200 Hz with a pulse width of 100 μ s. The radar frequencies currently used are near 7 and 14 MHz. The received sea echo signal is sampled at range gates chosen by the operator. An on-line computer performs the fast Fourier transform calculations of the sampled signals, and the resulting Doppler spectra are digitally recorded.

An electronic phase shifter monitored by the computer allows the monitoring of the sea echo from seven azimuths simultaneously. Lastly, the system is able to work at several frequencies simultaneously. The number of radar sea echoes that can be obtained during one experiment is the product of the numbers of frequencies, distances, and directions: these numbers can take any desired value in the limit of 28 for the product, corresponding to the current memory capacity of the computer.

The geographical situation of the radar and the directions of observation of the sea are shown in Figure 2; the corresponding bearings of the reception beams are 181°, 167°, 163°, 157°, 152.5°, 147°, and 133.5°, referred to geographical north. These values have been determined by electric field measurements at 2 km behind the array and over large ponds of salt water; they are reasonably near the expected theoretical values of 183°, 169.5°, 163.5°, 157.5°, 151.5°, 145.5°, and 133.5°.

A conventional meteorological station, in the neighborhood of the radar, gave the wind parameters, shown in Figure 3, during the period of experimentation. The sampling time is 1 hour (each sample represents an average over 1 hour). As can be seen, three main wind periods have been encountered with a speed greater than 16 kn (8.2 m/s): S/SSE from March 25 at 0900 to March 26 at 0800, with a speed up to 15 m/s; wind with the same direction from March 27 at 1200 to March 30 at 0600 and reaching 19 m/s; and wind from N/NNW from March 31 at 0600 to April 1 at 1500.

Thus the dominant wind directions correspond to radial winds blowing from either the shore (north winds) or the sea (south winds).

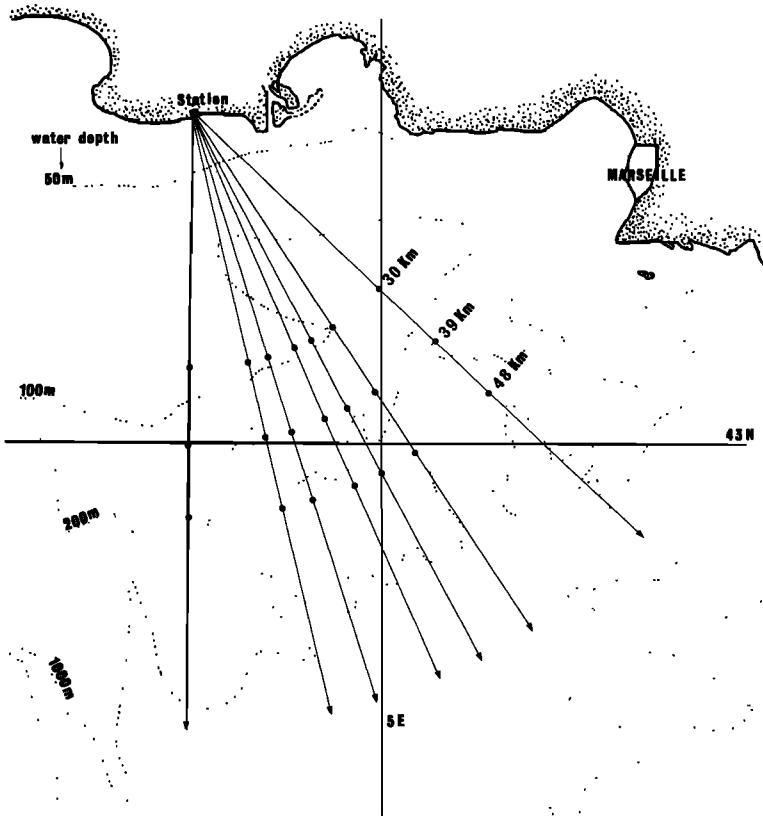


Fig. 2. Location of the radar station and directions of the radar beams.

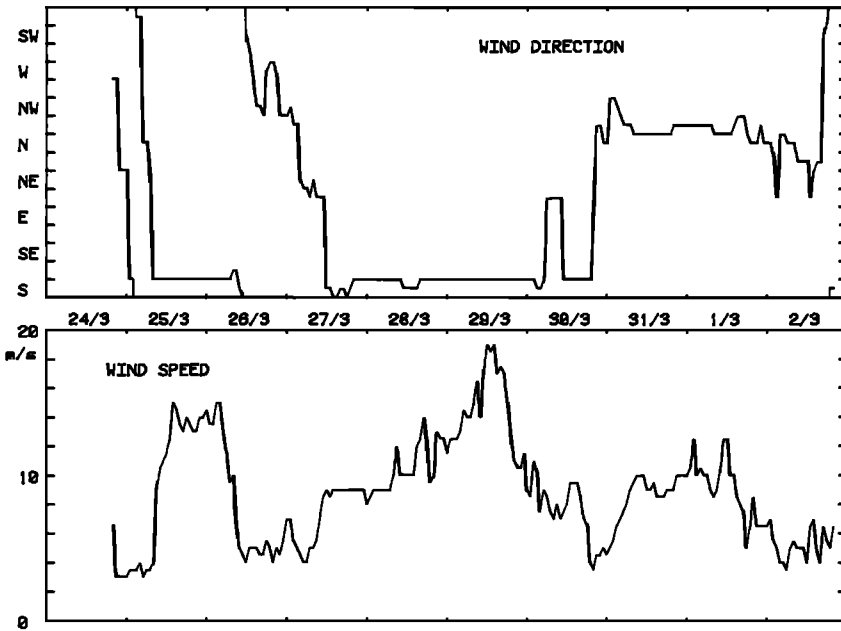


Fig. 3. Weather conditions encountered during the experiment.

TABLE 2. Doppler spectra characteristics for the two sets of experiments.

	3-hourly experiments	Specific distance- sounding experiments
Resolution	0.008 Hz	0.011 Hz
Sampling frequency	2.04 Hz	2.78 Hz
Number of incoherently averaged spectra	8	16
Global acquisition time	16 min, 44 s	24 min, 35 s

Two series of experiments have been carried out. The first one consists in collecting every 3 hours Doppler spectra of 21 radar sea cells simultaneously, placed at 30, 39, and 48 km along the seven reception azimuths allowed by the system. The radial extension of the cells is always 15 km. The sequence is performed at frequency $F1$ (near 7 MHz) and repeated just after at frequency $F2$ (near 14 MHz). These experiments, regularly repeated, allow the observation with a good continuity of the time evolution of the sea's spatial properties over the zone covered by the radar, between 22.5 and 55.5 km; they have also been used to measure ground wave attenuation, less precisely (since only three distances are considered) but more continuously in time than the second kind of experiments. During these latter, 14 sea cells are observed at two radar frequencies and in one direction. The distances typically lie between 15 and 93 km and are 6 km spaced; the radial length of the cells is still 15 km. The radiated power (1 kW for the peak power) was, for most of the time, not high enough to get sea echoes from more than 100 km. Such experiments were undertaken when weather conditions and the sea state homogeneity (estimated according to the last 3-hourly experiment) satisfied conditions 1 and 2 of section 3. A total of 10 such experiments have been made.

The characteristics of Doppler spectra corresponding to these two sets of experiments are shown in Table 2.

In order to increase the precision of spectral estimates for the 3 hourly experiments, the spectra corresponding to azimuths 167° , 163° , and 157° , on one hand, and 157° , 152.5° , and 147° , on the other hand, have been incoherently added together at every distance. This is justified by the fact that the associated radar cells are nearly adjacent and the Doppler spectra very similar. Extreme directions (181° and 133.5°) have not been considered.

5. EXPERIMENTAL RESULTS

5.1. *Attenuation rate measurements.* Here the results are given for specific distance-sounding exper-

iments. The corresponding wind conditions are listed in Table 3. The wind speed on the shore is always greater than 6 m/s and, for most of the time, comes from the south. The stability of radar and wind parameters is estimated as high enough to consider that the sea was homogeneous and in equilibrium with the wind all over the zone explored. Some experiments are associated with north winds, but soundings are done at distances far enough from the shore to expect that the fetch probably has no effect on the RCS, which therefore can be supposed to be constant; indeed, the results obtained do not significantly differ from those corresponding to south winds. Three examples of the signal attenuation with distance are shown in Figures 4a-c; the radar frequencies are 7 and 14 MHz, and the wind speed is 6.5, 10, and 13.5 m/s, respectively. The radar parameter plotted is $P_R \times R^3$ (dB), that is to say, following (3) in which σ is assumed to be constant, the relative monostatic Norton attenuation factor N_{mr} .

The data are least squares fitted by linear regression lines.

The theoretical curves of N_{mr} are also shown in the figure and refer to a smooth sea (N_{mr}^0). The difference between them and the experimental curves can be regarded as due to the sea roughness influence.

It appears at first that the scatter of the data around the regression lines is higher at 7 MHz than

TABLE 3. Wind parameters corresponding to distance-sounding experiments.

Time	Wind speed (m/s)	Wind direction (deg)
March 25, 1735	13	170
March 25, 2400	14.5	170
March 26, 0200	13.5	170
March 28, 0600	10	170
March 29, 0345	13	170
March 30, 0300	10	170
March 30, 1745	6.5	150
March 31, 1345	9.5	350
March 31, 2315	10	340
April 1, 0015	10	340

The wind direction angle is referred to the radar beam axis.

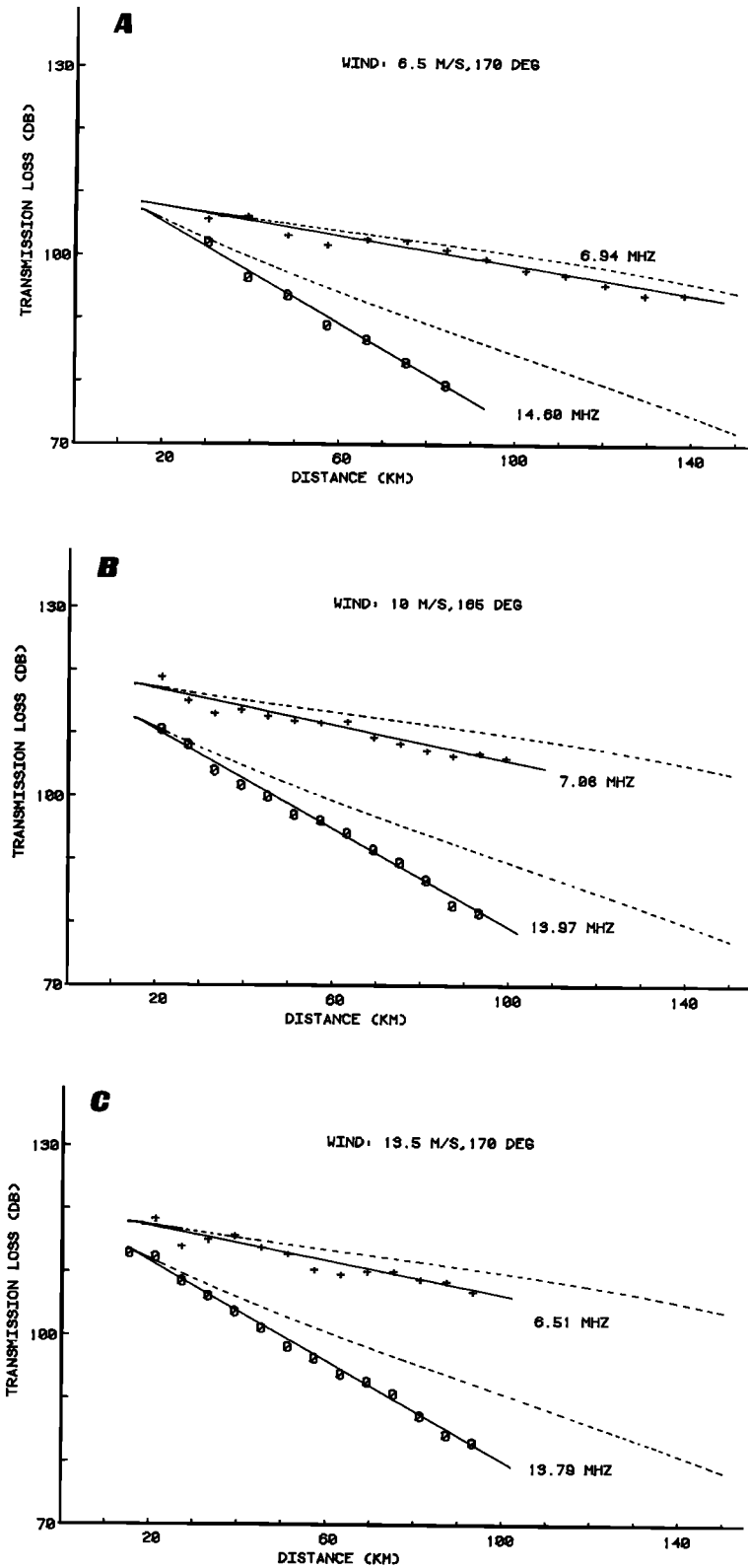


Fig. 4. Examples for various wind conditions of the monostatic Norton attenuation factor (relative); dashed lines represent its theoretical variation derived from Figure 1 and corresponding to a smooth sea.

at 14 MHz. This phenomenon exists regardless of the wind speed. It probably means that the spectral energy of the waves associated with 7 MHz (0.27 Hz) has a greater variability around the saturation value than for shorter waves associated with 14 MHz (0.38 Hz). A justification of that fact can be found in the work by Phillips [1977, p. 142] in terms of wave-wave interaction processes whose effect is to place the lower limit of the saturation range in the spectrum at frequencies significantly above the peak frequency; from that limit toward the peak, wave-wave interactions create energy transfers between waves, with different frequencies, causing distortions in the shape of the spectrum in such a way that a spectral form like the Pierson-Moskowitz is correct only if one considers the means in the temporal or spectral domain.

The slopes of the regression lines and for all the distance-sounding experiments are found to be -0.131 dB/km at 7 MHz (standard deviation = 0.010) and -0.415 dB/km at 14 MHz (standard deviation = 0.020).

The mean wind speed is 11 m/s with a direction roughly parallel to the radar beam. For similar wind conditions, the theoretical values are -0.128 dB/km at 7 MHz and -0.381 dB/km at 14 MHz by using the Phillips isotropic model for the sea state and -0.137 dB/km and -0.391 dB/km with a Pierson-Neumann (P-N) model (upwind/downwind). Taking into account the standard deviations of experimental data, the concordance is rather good between theoretical and experimental values of the rate of decay with distance of the monostatic Norton factor. Yet, no conclusion can be drawn about the variation of that rate with the wind speed, especially between 10 and 15 m/s, for the number of experiments is not high enough. Such a variation is investigated by the second kind of experiments.

5.2. *Variation of the attenuation rate with the wind speed.* The data from the 3-hourly experiments are considered now. Only the cases for which the wind is blowing from the south with a sufficiently high velocity and the Doppler spectra present similar ratios of the first-order lines at every distance have been retained in order to satisfy criteria 1 and 2 of section 3. The wind direction referred to the radar bearing lies between 150° and 220° .

Figure 5 shows the variation with the wind speed of the loss rate with distance of N_{mr} , say $\delta_{mr} = \Delta N_{mr} / \Delta R$ (in decibels per kilometer). The parameter δ_{mr} is derived from a linear regression be-

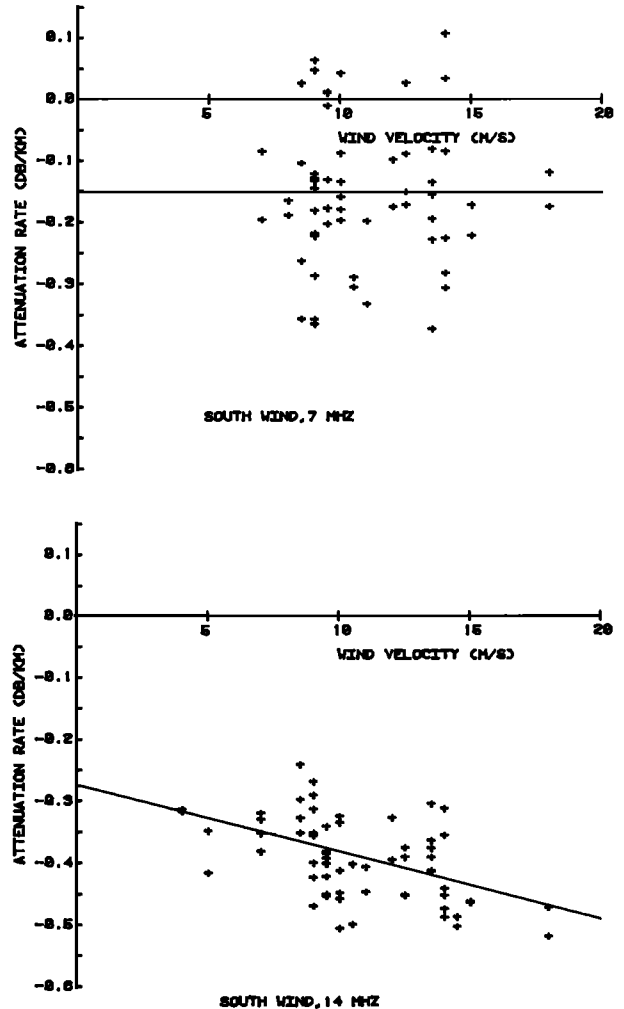


Fig. 5. Variation rate with distance of the monostatic Norton factor as a function of the wind speed, at 7 and 14 MHz; the wind is blowing from the south (fetch unlimited).

tween values of $P_R \cdot R^3$ at 30, 39, and 48 km and for two mean directions of the radar beam axis. Results obtained at both azimuth angles do not significantly differ, and they are plotted in the same figure. For 7 MHz the scatter of data is high, but it is smaller at 14 MHz. This should be considered in relation to what has been found out in section 5.1 concerning the first-order sea echo variability of the same order as that of ocean wave spectral energy. Moreover, loss rates are calculated from measurements obtained at only three distances (30, 39, and 48 km).

The regression lines fitting the data are given by

$$\begin{aligned} \delta_{mr} &= -0.0001U - 0.1503 & \text{at 7 MHz} \\ \delta_{mr} &= -0.0109U - 0.2733 & \text{at 14 MHz} \end{aligned} \quad (5)$$

with correlation coefficients equal to -0.0022 and -0.5047 , respectively.

There is no significant variation with the wind of δ_{mr} at 7 MHz. Barrick's simulation predicts values of δ_{mr} from -0.094 to -0.193 dB/km (upwind/downwind P-N model) or from -0.094 to -0.147 dB/km (Phillips isotropic model), for a wind speed between 0 and 15 m/s. So it is not surprising, given the scatter of measurements, that a deviation less than -0.1 dB/km (from 0 to 15 m/s) cannot be detected. Yet the mean value of the data, equal to -0.151 dB/km for a mean wind speed of 11 m/s, is reasonably close to the theoretical loss rate (around -0.13 dB/km) and also to the result of section 5.1 (-0.131 dB/km).

At 14 MHz, δ_{mr} clearly decreases with U . Table 4 shows the comparison between attenuation rates obtained from (5) and theoretical results. As can be seen, the agreement is good. From 0 to 15 m/s, δ_{mr} decreases to 0.164 dB/km, which rate is roughly the same as for the Phillips model (0.161 dB/km).

Given the lack of precision of the data, it is not possible to infer from these results which model for the sea state is the most convenient.

5.3. *Fetch influence upon the backscattered energy.* By ignoring the constraints involved by criterion of section 3 about the choice of the data periods to be considered, we examine here what happens when the wind is blowing from the north. In that situation the zone between the shore and the radar cells (including the radar cells themselves) lies in the wind wave generation area; then the sea can no longer be assumed a priori to be homogeneous, at least up to the cell at 48 km.

Figure 6 presents the variation of δ_{mr} with the wind speed, as derived from the data of the 3-hourly experiments, when the wind direction with respect to the radar direction is between -20° and $+20^\circ$. Wind speed is still greater than 4 and 6 m/s for 14 and 7 MHz, respectively. As for Figure 5 the data associ-

ated with the two azimuth angles have been gathered on the same plot.

The equations of the regression lines are

$$\begin{aligned}\delta_{mr} &= -0.0108U + 0.0649 & \text{at 7 MHz} \\ \delta_{mr} &= -0.0405U + 0.0795 & \text{at 14 MHz}\end{aligned}\quad (6)$$

The significant facts are (1) that the values of δ_{mr} are generally higher than for the previous case (south wind) and (2) that the slopes of the lines are more important. Some values of δ_{mr} from (6) in comparison with those from (5) and with theoretical ones are listed in Table 5.

The differences between the two sets of data are significant; they seem, especially for 14 MHz, to decrease as the wind speed increases; moreover, the north wind values of δ_{mr} differ notably from theoretical values with a tendency to approach them when the wind speed increases.

In fact, the quantity δ_{mr} represents the rate of the linear variation with distance of the Norton attenuation coefficient only if σ is constant. Returning to (3) and considering that the radar cross section σ is no longer constant, we find that

$$\delta_{mr} = \frac{\Delta (P_R \cdot R^3) \text{ dB}}{\Delta R} - \frac{\Delta \sigma \text{ (dB)}}{\Delta R} \quad (7)$$

so that δ_{mr} is explicitly affected by any variation of the RCS.

By comparison between the south and north wind values of δ_{mr} in Table 5, it is possible to find the variation with distance of the RCS in the north wind situation, which can be explained by an effect of the fetch: for a given wind speed, the RCS, proportional (following (2)) to $S(f_B) \cdot \phi(\theta)$, varies with the distance to the shore, supposed to be the fetch length.

If X is the fetch ($=R$) and ξ the nondimensional parameter gX/U^2 , the spectral energy of ocean waves of frequency f_B may be written as [Hasselmann *et al.*,

TABLE 4. Comparison of experimental and theoretical values of the attenuation rate δ_{mr} for various wind speeds at 14 MHz.

U (m/s)	δ_{mr} (dB/km)		
	Experimental values	Upwind/downwind, Pierson-Neumann	Cross wind, Phillips
0	-0.273	-0.257	-0.257
5	-0.328	-0.277	-0.303
10	-0.382	-0.373	-0.372
15	-0.437	-0.464	-0.418

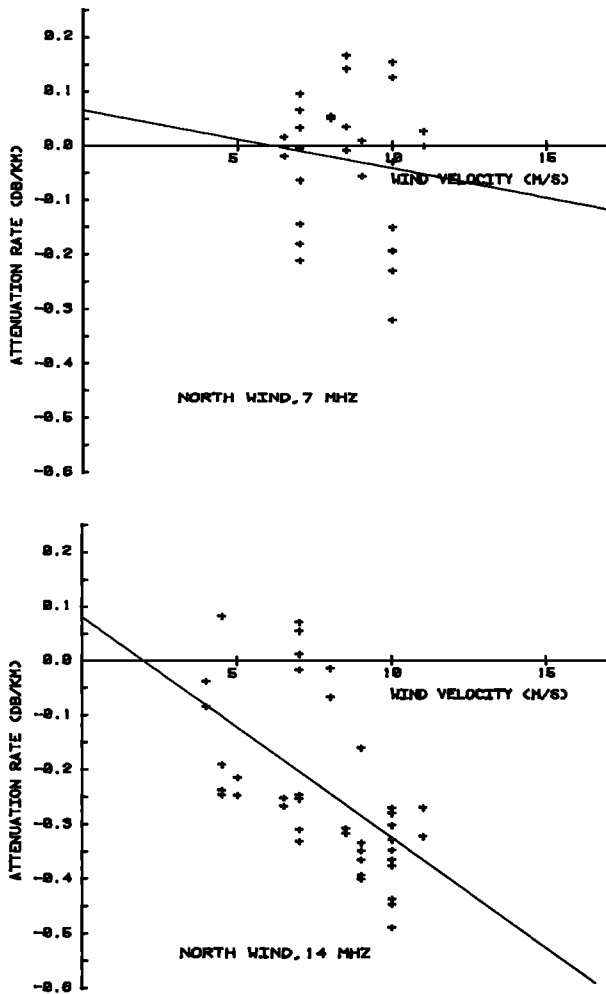


Fig. 6. The same as Figure 5 but the wind is blowing from the north (fetch limited).

1976]

$$S(f_B) = \frac{\beta_e g^2}{(2\pi)^4 f_B^2} \exp \left[-1.25 \left(\frac{F_m}{f_B} \right)^4 \right] \quad (8)$$

with

$$\beta_e = 0.076 \zeta^{-0.22}$$

$$F_m = 3.5(g/U) \zeta^{-0.33}$$

If the directionality factor ϕ is assumed to be constant, one obtains the increases of σ between 30 and 48 km presented in Table 6, which lists also the values of these rates derived from the experimental results in Table 5.

Results at 7 MHz are particularly convincing to explain the discrepancies between theoretical and experimental δ_{mr} in Table 5. This is not the case at 14 MHz, for which frequency the corresponding ocean waves are practically saturated from 30 to 48 km.

The fetch influences not only the RCS but also the sea state along the radio wave path. This could be evaluated precisely by a simulation of the transmission loss using a frequency spectrum like (8) which varies with the fetch length and so with the distance radar-to-target. This has not been done, but it is expected that the changes in transmission loss values due to this fact are more important at 14 MHz than at 7 MHz, since radio waves at 14 MHz are more sensitive to the sea state than the latter ones. The results at 14 MHz in Table 6 agree with this qualitative explanation. Yet, by assuming a variation of the RCS between 30 and 48 km to be the same as the theoretical one, the monostatic Norton coefficient is found to decrease with distance with slopes of -0.183 and -0.250 dB/km for wind speeds of 6 and 8 m/s, respectively, whereas the results of Table 4 give an order of magnitude of -0.3 dB/km for wind speeds lower than 5 m/s. The slopes found being significantly greater than this upper limit value, corresponding to a sea surface that is nearly smooth, the inhomogeneity of the sea state along the radar beam cannot explain entirely the discrepancies in the results at 14 MHz.

Lastly, if one assumes that Bragg waves are saturated at every distance, the directional parameter ϕ may vary with distance to the shore and with the wind speed. The RCS being proportional to ϕ , its

TABLE 5. Comparison of theoretical values of δ_{mr} (in decibels per kilometer) (Phillips isotropic model) with experimental values obtained by south and north winds, for various wind speeds and two radar frequencies.

U (m/s)	7 MHz			14 MHz		
	Theoretical (Phillips isotropic)	South wind	North wind	Theoretical (Phillips isotropic)	South wind	North wind
6	-0.097	-0.151	0.000	-0.317	-0.339	-0.164
8	-0.110	-0.151	-0.022	-0.344	-0.361	-0.245
10	-0.123	-0.151	-0.043	-0.372	-0.382	-0.326
12	-0.133	-0.152	-0.065	-0.390	-0.404	-0.407

TABLE 6. Difference due to a fetch effect between the radar cross sections at 30 km and 48 km, derived from Hasselmann's formulae (theoretical) and from experiments, for various wind speeds and two radar frequencies.

U (m/s)	$\sigma(48 \text{ km})/\sigma(30 \text{ km})$ (dB)			
	Values at 7 MHz		Values at 14 MHz	
	Theoretical	Experimental	Theoretical	Experimental
6	3	2.7	0.4	3.2
8	1.9	2.3	0.1	2.1
10	1.3	1.9	0	1.
12	0.9	1.6	0	-0.1

variations in Table 6 would mean that waves of frequency f_B become more directive as the fetch increases; indeed, the spectral energy of Bragg waves, under these conditions, increases with distance to the shore. In order to quantify this fact, consider the function

$$\phi = \cos^s \frac{\theta}{2} / N$$

where θ is the direction of propagation of Bragg waves with respect to the mean direction referred to as $\theta = 0$ and N is a normalization coefficient such that

$$\int_0^{2\pi} \phi(\alpha) d\alpha = 1$$

It is easy to show that the variations of σ between 30 and 48 km of Table 6 at 14 MHz correspond to variations of the parameter s of an order equal to 4.4, 2.6, and 1.6 for 6, 8, and 10 m/s, respectively.

All these causes act on the strength of backscattered signals, and it is impossible here to know the exact contribution of each of them on the actual results. Nevertheless, what is pointed out is the different nature of results obtained by south and north winds, which can be explained qualitatively by an effect of the fetch on the spectral energy of Bragg waves, on the radio wave path, and on directional properties of Bragg waves.

6. CONCLUSIONS

An HF monostatic experiment has been performed that estimates the ground wave attenuation as a function of distance and wind speed, at radar frequencies of 7 and 14 MHz.

A good agreement is found between theoretical and experimental results when the wind is blowing in

a direction parallel to the radar beam, with a velocity up to 38 kn (19.6 m/s).

Since no cross-wind situation (with a sufficiently high wind velocity) has been encountered, the sensitivity of the ground wave attenuation to the wave field orientation with regard to the radar beam azimuth has not been established. Besides the problem of evaluating the attenuation of radio waves with distance, an influence of the fetch on the strength of backscattered signals has emerged from the data. This suggests doing radar experiments with the specific goal of studying more precisely that influence.

Acknowledgments. This work has been supported by Centre National de la Recherche Scientifique under contract E.R.A. 668 and by Institut National d'Astronomie et de Géophysique under contract E 80.76.01. The authors are grateful to Joël Gaggelli for assuming the technical part of the radar station and to the society Les Salins du Midi for its logistic assistance during the experiments.

REFERENCES

- Barrick, D. E. (1970), Theory of ground wave propagation across a rough sea at dekameter wave lengths, *Tech. Rep. AD-865/840*, Battelle Memorial Inst., Columbus, Ohio.
- Barrick, D. E. (1971a), Theory of HF and VHF propagation across the rough sea, 1. The effective surface impedance for a slightly rough highly conducting medium at grazing incidence, *Radio Sci.*, 6(5), 517-526.
- Barrick, D. E. (1971b), Theory of HF and VHF propagation across the rough sea, 2, Application to HF and VHF propagation above the sea, *Radio Sci.*, 6(5), 527-533.
- Barrick, D. E. (1972), Remote sensing of sea state by radar, in *Remote Sensing of the Troposphere*, U.S. Government Printing Office, Washington, D. C.
- Forget, P., P. Broche, J. C. De Maistre, and A. Fontanel (1981), Sea state frequency features observed by ground wave HF Doppler radar, *Radio Sci.*, 16(5), 917-925.
- Frish, A. S., and B. L. Weber (1980), A new technique for measuring tidal currents by using a two-site HF Doppler radar system, *J. Geophys. Res.*, 85(3), 485-493.

- Hansen, P. (1977), Measurements of basic transmission loss for HF ground wave propagation over sea-water, *Radio Sci.*, 12(3), 397-404.
- Hasselmann, K., D. B. Ross, P. Muller, and W. Sell (1976), A parametric wave prediction model, *J. Phys. Oceanogr.*, 6(2), 200-228.
- Lipa, B. J., and D. E. Barrick (1980), Methods for the extraction of long-period ocean wave parameters from narrow-beam HF radar sea echo, *Radio Sci.*, 15(4), 843-853.
- Phillips, O. M. (1977), *The Dynamics of the Upper Ocean*, 2nd ed., 336 pp., Cambridge University Press, New York.
- Stewart, R. H., and C. Teague (1980), Dekameter radar observations of ocean wave growth and decay, *J. Phys. Oceanogr.*, 10(1), 128-143.
- Trizna, D. B., R. W. Bogle, J. C. Moore, and C. M. Howe (1980), Observation by HF radar of the Phillips resonance mechanism for generation of wind waves, *J. Geophys. Res.*, 85(C9), 4946-4956.